

Transport and Fate of Reactive Trace Gases in Red Spruce Needles. 1. Uptake of Gaseous Hydrogen Peroxide As Measured in Controlled Chamber Flux Experiments

Candis S. Claiborn*[†] and Viney P. Aneja[‡]

Laboratory for Atmospheric Research, Department of Civil and Environmental Engineering, Washington State University, Pullman, Washington 99164-2910, and Department of Marine, Earth, and Atmospheric Sciences, North Carolina State University, Raleigh, North Carolina 27695-8208

Foliar uptake by plants represents an important sink for many air pollutants. In this, the first of two companion papers, a continuous-flow, well-mixed exposure chamber was used to study the fluxes of gaseous hydrogen peroxide to red spruce saplings. Wall losses were found to be substantial and highly variable, requiring frequent wall loss measurements throughout the course of the experiments. No significant difference was observed between daytime and nighttime losses of hydrogen peroxide to the needle branches. The pseudo-second-order reaction rate constant describing the flux to the needle surface was calculated to be 0.35×10^{-4} ($\pm 31\%$) $\text{cm}^{-2} \text{min}^{-1}$ during daytime exposure (PAR = $400 \mu\text{Einstein m}^{-2} \text{s}^{-1}$ with grow light on), and 0.32×10^{-4} ($\pm 39\%$) $\text{cm}^{-2} \text{min}^{-1}$ during the night (PAR = $0 \mu\text{Einstein m}^{-2} \text{s}^{-1}$ with grow light off). The corresponding deposition velocities as determined from the slope of the line when the flux is plotted as a function of concentration were 0.09 cm s^{-1} for both day and night conditions. It is inferred from these experiments that foliar uptake of hydrogen peroxide by red spruce appears to be limited to surface deposition only. In the following paper in this issue, these data are analyzed using a detailed model describing gas transport.

I. Introduction

Red spruce/Fraser fir forests in the Appalachian Mountains have exhibited high rates of decline and mortality and have been the subject of a number of investigations (1-4). Atmospheric deposition of acidic precipitation or toxic gaseous pollutants such as ozone has been considered as a potential stress contributing to the observed forest decline. Although not yet implicated in the decline of spruce/fir forests in the Appalachians, exposure to atmospheric ozone has been found to cause damage to other coniferous forests, such as ponderosa pine in southern California and white pine in the eastern United States (ref 5, and references cited therein).

Atmospheric hydrogen peroxide is a photochemical oxidant similar to O_3 in that it is a strong oxidizing agent. Tropospheric concentrations tend to be on the order of 0.5-5 ppb or 1-2 orders of magnitude lower than those of O_3 (ref 6 and references cited therein, 7). The Henry's law constant for H_2O_2 is on the order of $10^5 \text{ mol L}^{-1} \text{ atm}^{-1}$ (8) compared to 10^{-2} for O_3 (9); therefore, although it is much less concentrated in the atmosphere than O_3 , H_2O_2 is considerably more water-soluble so that its potential for damage to sensitive inner plant tissues, which are composed mainly of water, may be as great as or greater than

that of O_3 . (It is worth noting here, however, that in the following paper we will show that, for two sets of experiments, it does not appear that H_2O_2 reached the inner tissues.) The results of preliminary studies, in which Norway spruce specimens were exposed to acidic mist containing hydrogen peroxide in typical precipitation concentrations, suggest that such exposure could cause foliar damage (11). In another study during which red spruce was simultaneously exposed to gaseous H_2O_2 , O_3 , and SO_2 , enhanced respiration was observed to occur (12). The results of a third study showed no effects on red spruce from the exposure of mist containing H_2O_2 (13).

Foliar uptake by plants represents an important sink for many air pollutants, yet factors for characterizing pollutant uptake rates that are used in regional atmospheric chemistry models are currently applied with a large degree of uncertainty. For gaseous H_2O_2 , deposition to vegetation canopies may represent a major sink, since H_2O_2 is very water-soluble and reactive. Consideration of atmospheric H_2O_2 is important when studying atmospheric oxidants and radical budgets; therefore, parametrization of its deposition is necessary for modeling studies. Yet few measurements of deposition rates of H_2O_2 , either in field experiments (14) or in controlled laboratory experiments (12), have been reported.

In order to resolve whether atmospheric H_2O_2 can be injurious to spruce (or other conifers), there is a need to better understand the exposure of conifers from a mechanistic viewpoint. In the work described in this and in a companion paper (10), the transport and fate of gaseous H_2O_2 into needles of red spruce were investigated using a well-mixed, continuous-flow exposure chamber (MFC). The purpose of the work described in this paper is to determine the flux of gas-phase atmospheric H_2O_2 to red spruce saplings in controlled exposure chamber experiments and to examine the sensitivity of the flux to varying environmental conditions (such as available light or varying concentrations). Most uptake studies have been conducted on insoluble gases such as NO_2 or O_3 , or on moderately soluble gases such as SO_2 . Handling labile and/or water-soluble gases such as H_2O_2 requires additional care to minimize wall losses so that the fluxes to plant species can be observed. The chamber constructed for this work was specially designed for use in flux experiments on reactive gases. In Claiborn et al. (10), the results of these experiments are interpreted from a theoretical basis, and the fate of gaseous H_2O_2 in red spruce is examined.

II. Experimental Apparatus and Methods

Exposure Apparatus. The MFC design has been used extensively in exposure experiments because when the chamber is well-mixed, the conditions inside are uniform throughout, and the exit conditions are representative of

* Author to whom correspondence should be addressed.

[†] Washington State University.

[‡] North Carolina State University.

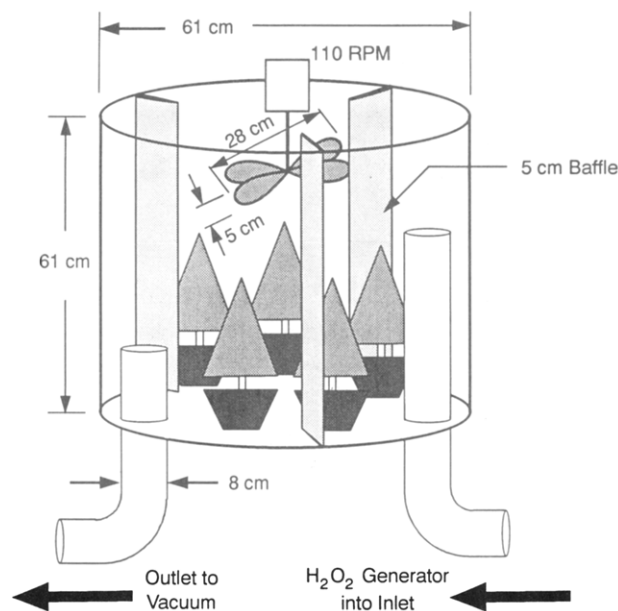


Figure 1. MFC used in experiments. Chamber volume, 178 L. Impeller speed, 110 rpm. All surfaces were Teflon-coated.

the internal conditions (15). This feature of the MFC design greatly simplifies calculational procedures of fluxes and mathematical treatment of wall losses and facilitates understanding and quantifying the exposure of the plants in the chamber. Moreover, the resistance calculated from the exposure chamber experiment is useful for understanding the fate of pollutants in their natural settings. A MFC was constructed with dimensions of 61 cm in height by 61 cm in diameter (Figure 1) to give a 1:1 diameter to height ratio, which is ideal for the MFC (16). During an experiment, the chamber contained between two and four whole spruce saplings. The chamber itself consisted of a minimal Teflon-coated support frame covered by clear Teflon film. Mixing was provided by an impeller (110 rpm) mounted at the top of the chamber and three vertical baffles. The chamber inlet, outlet pipes, and all sample ports were constructed out of Teflon. The chamber flow rate was set to achieve gas residence times of 1–2 min. Gas-phase H_2O_2 was generated using a Henry's law generator (8). The sample source was switched between the chamber inlet and outlet on a 15-min basis, so that the sample duration was 15 min.

Light to the chamber was provided by a GE Model 85 MV 400/U 400-W multivapor light that was installed approximately 3 ft above the top of the chamber. Measurements of photosynthetic photon flux density (PPFD), a measure of the photosynthetically active radiation (PAR), indicated that the PPFD at branch level (approximately $400 \mu\text{Einstein m}^{-2} \text{s}^{-1}$) was similar to or lower than that used in other studies [Ennis et al. (12) reported PAR of approximately $600 \mu\text{Einstein m}^{-2} \text{s}^{-1}$]. We also found that significant shading occurred between the top branches and the floor (PAR was approximately $200 \mu\text{Einstein m}^{-2} \text{s}^{-1}$ at floor level). The role of light gradients in forests has been discussed by Baldocchi et al. (17) who have incorporated this aspect into their modeling work.

Mixing Characteristics. Mixing studies were conducted using nitric oxide (NO) as the tracer gas (7). NO was introduced to the chamber from a cylinder of 100 ppm NO, and the chamber response to this step change in NO was measured using a Monitor Labs Model 8440 analyzer. The response time of this analyzer was very fast and, therefore, was neglected. Losses to the chamber wall were

also negligible. Step tests were conducted on both the empty chamber and the chamber plus two spruce saplings and were conducted at 85, 142, and 184 slpm, and all tests were repeated at least twice. The effective chamber volume for the empty chamber as determined from these studies ranged from 70 to 90% of the actual volume, so that the "dead volume" (in which poor or no mixing occurs) for the empty chamber is roughly 10–30% of the total chamber volume. The effective chamber volume for the chamber filled with two trees was approximately 60% of the actual chamber volume. It appears that the trees contribute to the nonideal behavior of the chamber by providing an additional dead volume equal to roughly 15–30% of the total chamber volume. This estimated dead volume seems reasonable based on visual observation of the amount of space occupied by the trees.

Biological Materials. Seedlings started from seeds of red spruce growing in the Mt. Mitchell, NC, forest were obtained in July 1989 from the U.S. Forest Service's Northeastern Forest Experiment Station in Durham, NH. The seedlings were maintained in the NCSU phytotron greenhouse (18). Before the flux experiments were commenced, the trees were forced into budbreak by exposing them to cold temperatures and shortened photoperiods for several weeks.

Experimental Methods. The experimental portion of this investigation consisted of three activities: chamber wall losses were examined, then H_2O_2 fluxes to red spruce saplings were measured in the exposure chamber, and finally leaf area was measured for all subject plants.

Wall Losses. Wall losses of gaseous H_2O_2 were measured at the beginning, at the end, and frequently throughout the experiments. Wall losses were measured at varying residence times, at a range of chamber concentrations, and during both nighttime (PAR = 0) and daytime (PAR = $400 \mu\text{Einstein m}^{-2} \text{s}^{-1}$ at branch level) conditions. During the actual flux experiments, the pots of each tree were placed in plastic Ziploc bags that were secured around the trunk of the tree. At the end of each experimental run, the trees were removed from the chamber, and wall loss experiments were again performed. H_2O_2 losses to the Ziploc bags were not measured but based on the relative areas of the bags and the chamber wall, losses to the bags were assumed to be negligible compared to chamber wall losses (the exposed Ziploc bag area was approximately 5% of the chamber wall area).

Flux Experiments. Flux experiments were run both with and without light and at varying concentrations of pollutants. The duration of the experiments was varied in order to determine if steady state was rapidly achieved; however, in general the trees were not left in the chamber for more than approximately 3 days. During flux experiments, the air flow rate and inlet and outlet conditions of temperature, carbon dioxide, water vapor content, and H_2O_2 concentration were monitored. Samples from the chamber inlet and outlet were analyzed for CO_2 using an Anarad AR-500R infrared CO_2 analyzer. Water vapor content was measured using an EG&G Model 880 dewpoint hygrometer. To measure H_2O_2 , a dual-channel enzyme fluorescence analyzer was used (19). The level of detection of the instrument is 0.1 ppb. Calibrations were performed daily against aqueous-phase standards that were also made up daily by serial dilutions of 30% H_2O_2 solution. The H_2O_2 stock solution was checked at least weekly by titration against KMnO_4 solutions, which in turn were titrated against a standard $\text{Na}_2\text{C}_2\text{O}_4$ solution. The uncertainty of

these calibrations as described by the 95% confidence interval when all calibrations were considered was $\pm 10\%$ at the 5 ppb level. Calibrations were not checked against gas-phase calibrations; however, we assume the collection efficiency from gas phase to aqueous phase was complete since the instrument was operated within the recommended operating range of flow rates and reagent pH values. All concentration data were continuously recorded on chart paper and extracted as 15-min averages. The air flow rate through the chamber was measured by rotameter and controlled manually. The temperature inside the chamber was monitored using a Bailey BAT-12 thermocouple.

Leaf Area Measurements. Leaf area of the spruce needles was estimated using a projected area technique (optical planimeter) and by measuring the needle number density, length, and cross-section dimensions of needles and branches. A glass bead technique was also attempted to estimate leaf area (20–22); however, the results of this technique were highly variable. Therefore, these results were not utilized for calculating fluxes.

To convert the projected area measured by the planimeter to a total leaf area, the planimeter reading must be multiplied by some geometric factor. Since spruce needles contain stomata on all sides and since the cross-section of a red spruce needle is four-sided, the planimeter reading was multiplied by a factor of 4. The actual factor may be somewhat lower. For example, Ennis et al. (12) reported that the actual needle area as estimated from a glass bead technique for red spruce was 2.75 times the projected area.

To calculate the leaf area from needle dimensions, all branches were removed, classified according to degree of branching, and measured. Needles were also removed, counted, and measured for several lengths of branches. Cross-sectional cuts were made in randomly selected needles, and these were observed under the microscope for dimensions. The total leaf area calculated from this technique for four trees were 8331, 7563, 8697, and 5706 cm^2 for trees 1–4, respectively. The estimated error for these measurements is 25%. The estimates from this technique and from the optical planimeter using a factor of 4 were within approximately 30% of each other.

Computational Methods. All concentration data were extracted as 15-min averages. Since only one analyzer was available for measuring both inlet and outlet concentrations, it was impossible to obtain simultaneous measurements of chamber inlet and outlet concentrations. In order to calculate concentration differences between the inlet and outlet, "running averages" were obtained by linearly interpolating between measurements. The concentration difference was then obtained by taking the difference between a measured 15-min average and the corresponding running average. This method resulted in four measurements of concentration difference per hour except for the first and last hour of the experimental run, during which only three differences were obtained. A single flux calculation was determined for each 15-min concentration difference obtained. For each run, an average flux was determined by calculating the mean and standard deviation of these 15-min flux calculations.

Following the nomenclature described in Ennis et al. (23), the fractional loss of H_2O_2 to the chamber walls, CL (unitless), is defined as the fraction of inlet H_2O_2 which is lost to the walls during the chamber loss experiment (24). For experiments measuring the uptake by vegetative species, the total loss of H_2O_2 to all surfaces, TL (the

fraction of entering H_2O_2 which is lost to all surfaces during the experiment, unitless), is similarly calculated. The amount of H_2O_2 which is lost to the branches only (BL) is calculated from TL and CL by assuming that ideal mixing occurs in the chamber and that the uptake by trees and losses to walls act as two parallel reactions (24). Then, the fractional loss to the branches can be calculated from the total fractional loss and the chamber loss (23, 24)

$$\text{BL} = \frac{(\text{TL} - \text{CL})}{(1 - \text{CL})} \quad (1)$$

The flux of H_2O_2 to branches (Q_A , $\text{mol cm}^{-2} \text{min}^{-1}$) is calculated from the fractional loss to branches, chamber airflow rate (F , slpm), inlet H_2O_2 concentration (C_{A_0} , ppb), and estimated total needle surface area (A_L , cm^2)

$$Q_A = \frac{(\text{BL})(F)C_{A_0, \text{exp}}}{A_L} \times \text{conversion factors} \quad (2)$$

A pseudo-first-order reaction rate constant (k_2 , min^{-1}) describing the loss of H_2O_2 to the branches can also be calculated from the branch loss (BL), the total loss, (TL), and the chamber residence time (τ , min) (24)

$$k_2 = \frac{\text{BL}}{\tau(1 - \text{TL})} \quad (3)$$

Assuming that the intercellular concentration is zero and that the chamber contents are well-mixed so that the exit concentrations are indicative of the chamber concentrations, then the deposition velocity (V_d , cm s^{-1}) defined as the inverse of the mass-transfer resistance (25) can be calculated from the relationship

$$V_d = \frac{Q_A}{C_{A, \text{exp}}} \times \text{conversion factors} \quad (4)$$

where $C_{A, \text{exp}}$ is the outlet H_2O_2 concentration for the flux experiment and Q_A is the flux of H_2O_2 to the leaf surfaces. It should be pointed out that the deposition velocity calculated from these experiments is not the same as that measured in the field. The field deposition velocity includes terms that take into account the resistances due to atmospheric, pollutant, and leaf boundary layer characteristics (25). Because of the well-mixed characteristics of the MFC, there should be little aerodynamic resistance, and the boundary layer resistance should be also minimized. Moreover, the deposition velocity measured in an actual canopy would include contributions from deposition to nonvegetative surfaces (for example, soils or rocks).

For determining statistical significances in the following sections, F -test calculations were performed. Unless otherwise noted, statistical significance at the 95% confidence level was computed.

III. Results

Wall Losses. Extensive wall loss measurements were made throughout the chamber experiments. Wall losses were found to range, depending on the chamber flow rate, from 10 to 33% of the inlet H_2O_2 during the day and from 4 to 14% at night. Because the wall loss experiments were conducted at varying chamber flow rates, the pseudo-first-order reaction rate constants rather than the fraction loss (CL) should be compared for all experiments (Figure 2). The wall loss rate constants (k_1) were found to be highly variable (overall standard deviation approximately 50% during days; >35% at night) and were much higher during periods with the light on compared to periods when the

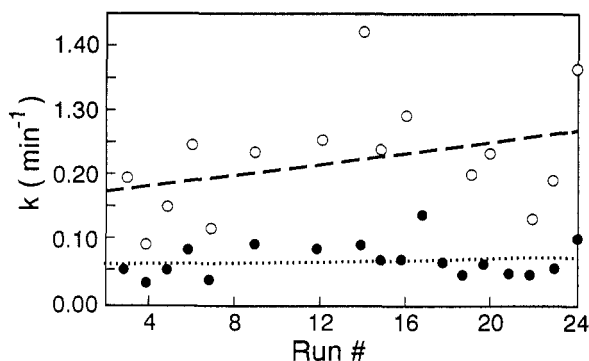


Figure 2. Chronology of wall losses. Open circles denote daytime experiments; filled circles denote nighttime. The wall loss rate constant was relatively constant during the dark runs throughout the course of the experiments, while the daytime rate constant was highly variable and appeared to be increasing through the experiments.

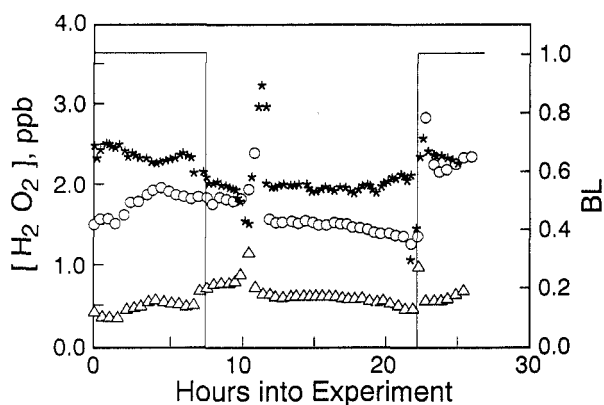


Figure 3. Branch loss data from run number 3c. Inlet (open circles) and outlet (open triangles) H_2O_2 concentrations and calculated fractional branch losses (*) as a function of time. Solid line indicates light on at value of 1, light off at value of 0. Run 3c, April 1991; trees 1-4; chamber air rate, 142 slpm.

light was off ($k_1 = 0.245 \pm 0.122 \text{ min}^{-1}$ and $k_1 = 0.070 \pm 0.026 \text{ min}^{-1}$ when light was on and off, respectively). This is consistent with the observations of Ennis et al. (23), who also noted that the H_2O_2 chamber losses were significantly higher during light-on than during light-off conditions.

H_2O_2 Uptake by Spruce. Uptake experiments were conducted on three groups of spruce saplings. The earlier runs (1-12) were conducted on four trees (trees 1-4) placed in the chamber. Runs 13-15 and 25-31 were conducted on trees 1 and 2, and runs 16-24 were conducted on trees 3 and 4. As an example, the chronology of run 3 and the accompanying temporal variation of the fractional loss of H_2O_2 to branches are shown in Figure 3. In this figure, there are two excursions in the inlet H_2O_2 concentration. Flux calculations were made based on steady-state conditions; therefore, the "spikes" in H_2O_2 concentration were not taken into account in calculating the average H_2O_2 concentrations in the inlet and exhaust and were also not included in the flux calculations. A summary of operating conditions, including exposed leaf area, residence time, inlet H_2O_2 and CO_2 concentrations, and outlet dewpoint temperature, is given in Table I. In all, 31 experimental runs were conducted (24), of varying duration, ranging from 4 h to as long as 67 h for one experiment (run 2). In general, the earlier runs were allowed to proceed for longer durations than the later runs until it was determined that the length of time could be shortened per run without any substantial loss of information. Dewpoint temperatures during these experiments ranged from 7.8 to 17 °C during

Table I. Summary of Operating Conditions for Chamber Flux Experiments, Measuring Fluxes of Gas-Phase Hydrogen Peroxide to Red Spruce Surfaces^a

runs	A_L (cm ²)	τ (min)	$[\text{H}_2\text{O}_2]_{in}$ (ppb)	$[\text{H}_2\text{O}_2]$ sd (%)	T_{dout} (°C)	$[\text{CO}_2]_{in}$ (ppm)
1-12	30 297	1.3-1.6	0.79-8.25		7.9-17.8	
13, 23-28	15 894	1.3-2.1	2.80-9.72		17 ± 1 (d)	16 ± 1 (n)
14-22	14 403	1.0-2.1	2.08-9.37		17 ± 1 (d)	16 ± 1 (n)
summary		1.0-2.1	0.79-9.72	12.9 (d) 14.2 (n)	7.9-18.0	450 ± 50 (d) 390 ± 30 (n)

^a A_L is the leaf area; τ is the residence time; $[\text{H}_2\text{O}_2]$ and $[\text{CO}_2]$ denote hydrogen peroxide and carbon dioxide concentrations, respectively; T_d is the dewpoint temperature; (d) and (n) denote day and night, respectively; and the subscripts *in* and *out* denote inlet and outlet conditions, respectively.

runs 1-12 and were reasonably constant at 17 ± 1 °C (daytime) and 16 ± 1 °C (nighttime) in runs 13-231. CO_2 concentrations were variable, ranging from 350 to 500 ppm and averaging 450 ± 50 ppm during the day and 390 ± 30 ppm at night. The average CO_2 flux was $2.31 \pm 0.71 \times 10^{-9} \text{ mol cm}^{-2} \text{ s}^{-1}$ during the day and $-1.54 \pm 0.83 \times 10^{-9} \text{ mol cm}^{-2} \text{ s}^{-1}$ at night.

IV. Discussion

Wall Losses. There are several factors which may contribute to the increase in wall losses when the light is on. The first factor may be the presence of the light itself. H_2O_2 is known to photolyze to some extent in the atmosphere (e.g., ref 26). A second factor may be the increased chamber temperature when the light is on, although the temperature difference was not substantial; the chamber temperature was 25.0 °C when the light was on and 22.5 °C when the light was off. A third factor may be the presence of residual biogenic hydrocarbons emitted from the trees which have adsorbed onto the chamber walls and which may also react in the presence of light to form hydroxyl radicals that in turn may react with H_2O_2 . The possible role of biogenic hydrocarbon emissions may also explain in part why the daytime wall losses (evidenced by the wall loss rate constant) appeared to increase throughout the course of the experiments (Figure 2). Particularly in the earlier experiments (runs 1-7), the wall losses tended to be highly variable. In the later experiments, the wall losses varied inversely (significant at the 95% level) with concentration (Figure 4).

Although the reaction at the wall was assumed to be first order with respect to H_2O_2 , in the later experiments (runs 9-13) the rate "constant" was observed to be negatively correlated to the chamber H_2O_2 concentration, particularly during daytime conditions (Figure 4). The rate constant appears to be proportional to the H_2O_2 concentration raised to a fractional power; a plot of the $\ln(r_A)$ vs $\ln([\text{H}_2\text{O}_2])$ suggests an exponent of -0.56 to -0.57 ($r^2 = 0.87$) for both day and night conditions (Figure 5). A noninteger order in the rate law suggests the presence of intermediate species in the reaction mechanism (27). Since the concentration dependence of the decomposition rate constant is evident only for the daytime wall loss data, we investigated the possibility that the decomposition of H_2O_2 is accelerated during the day due to the photolytic formation of hydroxyl radicals with which H_2O_2 is known to react (28). An examination of the fraction of H_2O_2 lost due to gas-phase reaction with OH radical using published

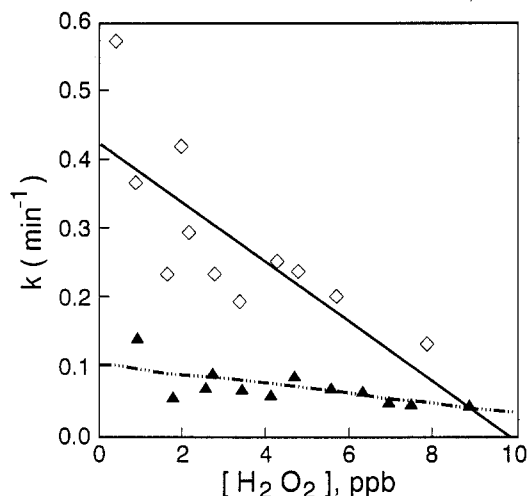


Figure 4. Pseudo-first-order rate constant for wall losses as a function of chamber concentration. Filled triangles denote nighttime experiments; open diamonds denote daytime experiments. Pseudo-first-order rate constant, k , is shown to be dependent on the chamber hydrogen peroxide concentration. k is in units of min^{-1} . Data taken from runs 9 and later.

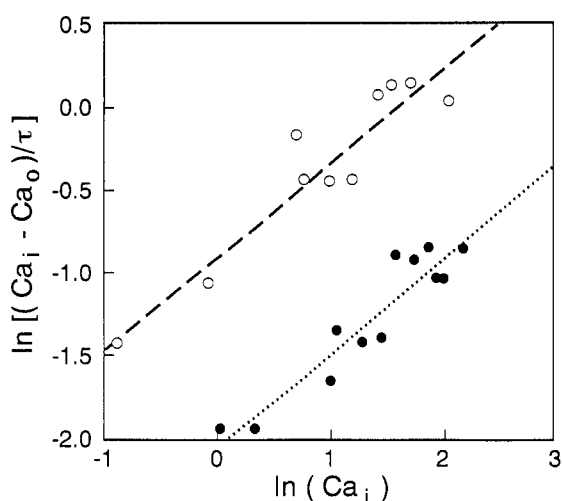


Figure 5. Pseudo-first-order wall loss rate as function of chamber H_2O_2 concentration. Open circles denote daytime experiments; filled circles denote nighttime. C_{ai} and C_{ao} denote inlet and outlet H_2O_2 concentrations, respectively (ppb). τ is the chamber residence time (in min). r^2 is 0.87 for night and 0.88 for day. A fractional power of -0.56 to -0.57 is suggested for "reaction" order. Average k is $0.131 \pm 0.020 \text{ min}^{-1}$ (nights) and $0.412 \pm 0.078 \text{ min}^{-1}$ (days).

reaction rate constants (29), however, suggests that, at the residence times used for these experiments, this pathway would not contribute to the H_2O_2 losses to a great extent. Similarly, neither photolysis of H_2O_2 nor aqueous-phase reaction with OH should account for more than approximately 2% of the measured losses. Without more information on the reaction kinetics of heterogeneous decomposition of H_2O_2 , it is not possible at this time to specify the reason for the higher wall losses during the day.

Throughout the course of our experiment, the daytime wall losses appeared to increase. This apparent increase, however, is not significant at the 95% level, but is at the 90% level. Ennis et al. (23) also noted that the wall loss increased during the course of their experiments. This phenomenon may be due to emissions from biological materials (e.g., biogenic hydrocarbons or their byproducts) coating the chamber walls as mentioned above or to the conditioning of the walls as plasticizer additives are

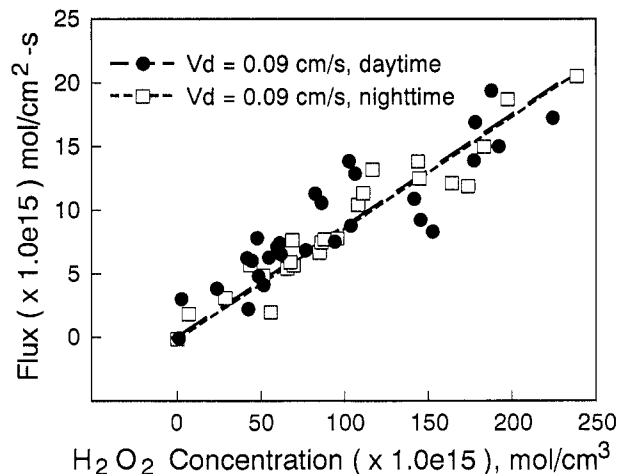


Figure 6. H_2O_2 flux to red spruce as a function of concentration. Filled circles denote daytime runs; open squares denote nighttime runs. The average deposition velocity was determined from the slope of the above lines when they are forced through the origin ($V_d = Q/C$ where Q is the flux (in $\text{mol cm}^{-2} \text{ s}^{-1}$) and C is the concentration (in mol cm^{-3}).

volatilized from Teflon. When dealing with gaseous oxidants in Teflon bags, for example, the surfaces of the Teflon film are generally conditioned before use. It is speculated that, during this conditioning, either the volatilizing materials previously mentioned are being displaced by permeating water vapor or other polar gases or the active sites on the surfaces of the film are becoming oxidized. Usually, the effect of conditioning is that the film becomes less reactive (e.g., with O_3) rather than becoming more reactive, as is apparently the case for H_2O_2 . In both our experiments and in those of Ennis et al., it is not known whether the changing wall reactivity was due to the presence of biological materials in the chamber or due to extended exposure of the chamber surfaces to H_2O_2 since empty control chambers were not operated. Since the wall losses were so variable and not well-understood, we found that it was important to continually monitor this parameter.

Fluxes, Rate Constants, and Deposition Velocity.

Average fluxes were calculated for each run conducted on red spruce (24). A linear relationship between the flux and chamber concentration emerged that was consistent with the empirical deposition model of eq 4 (Figure 6). The deposition velocity and pseudo-second-order rate constant (k'_2) was calculated for each experiment and a summary is given in Table II. In developing this table, the second daytime experiment (run 2 in this manuscript) was not included because the outlet H_2O_2 concentration measured was below the level of detection for the instrument. The average deposition velocity calculated from each run on red spruce (range 0.08 – 0.12 cm s^{-1} and 0.08 – 0.12 cm s^{-1} for days and nights, respectively) is plotted against the run sequence number in Figure 7. The deposition velocity remains relatively constant throughout the experiments and between the different groups of trees (0.096 ± 0.038 and $0.090 \pm 0.019 \text{ cm s}^{-1}$ for average daytime and nighttime deposition velocities, respectively). As determined from the slope of a plot of the flux versus the H_2O_2 concentration when the line is forced through the intercept, the deposition velocity is 0.09 cm/s for both day and night (Figure 6).

Linear regressions were calculated for the daytime data, nighttime data, and the entire data set (Figure 6). When an F -test is used to examine the statistical significance, there is no significant difference at the 95% level in these

Table II. Summary of Reaction Rate Constants^a and Deposition Velocities for Hydrogen Peroxide to Red Spruce

expl runs	$k'_2 \times 10^4$ ($\text{cm}^{-2} \text{min}^{-1}$)	V_d (cm s^{-1})	comment
runs 1-12	0.40 ± 1.01	0.11 ± 0.06	day, trees 1-4
	0.38 ± 0.20	0.12 ± 0.03	night, trees 1-4
runs 13-15,	0.36 ± 0.10	0.089 ± 0.013	day, trees 1 and 2
25-31	0.30 ± 0.05	0.11 ± 0.030	night, trees 1 and 2
runs 16-24	0.26 ± 0.05	0.085 ± 0.010	day, trees 3 and 4
	0.29 ± 0.03	0.076 ± 0.014	night, trees 3 and 4
summary	0.35 ± 0.11	0.10 ± 0.04 (0.09) ^b	day, all experiments
	0.32 ± 0.13	0.09 ± 0.02 (0.09) ^b	night, all experiment
Ennis et al.		0.37 ± 0.03	day
		0.33 ± 0.01	night

^a k'_2 is the pseudo-second-order rate constant describing the flux to the leaf surfaces. V_d is the deposition velocity. ^b Value in parentheses is that calculated from the slope of the line, shown in Figure 6.

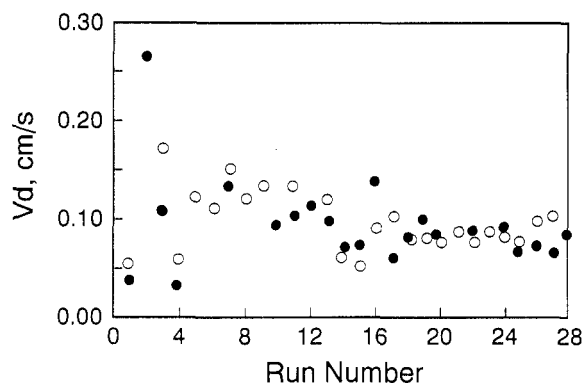


Figure 7. Deposition velocity calculated from each run for red spruce saplings in chronological order. Filled circles denote nighttime runs; open circles denote daytime runs.

experiments between nighttime and daytime H_2O_2 fluxes to red spruce. A diurnal variation in fluxes is observed for many plant types and for several other air pollutants, such as O_3 or nitrogen species (e.g., refs 30 and 31). Ennis et al. (12) also observed no diurnal variation in fluxes of H_2O_2 to spruce and concluded that H_2O_2 deposits on the outer surfaces of the needles and does not reach the stomata, which would otherwise affect the flux at night as the stomata close. Results of preliminary resistance calculations (32) indicate that the porous stomatal antechamber that is above the stomatal opening on spruce needles provides an extra resistance to gas exchange that is absent in the broadleaf plant, whose stomata are on the surface of the leaf. In Claiborn et al. (10) we discuss how this stomatal "plug" affects plant gas exchange, based on fundamental modeling studies simulating the experiments presented here. We speculate, on the basis of these experimental results and the modeling studies that, in these experiments, gaseous H_2O_2 did not reach the inner regions of the spruce needle but was deposited on the surface and perhaps in the porous antechamber. Since many broadleaf plants have their stomata on the leaf surface, further experimentation is warranted to determine if the flux of H_2O_2 to broadleaf plants is controlled by stomatal responses to light.

Comparison to Other Measurements. Deposition velocities have been calculated using a mixed flow enclosure chamber by a number of investigators for agronomic plants and for forest species. Taylor et al. (33) investigated the deposition velocity of several sulfur-containing trace gases to various agronomic plants and found that the deposition velocity increased with increasing water solubility. Am-

monia, which is very water-soluble, was found to have a relatively high deposition velocity to several crops during the day but not at night (30). Ennis (34) reported that, in their study, the water-soluble gases (H_2O_2 and SO_2) demonstrated little difference between nighttime and daytime deposition velocity, and in fact, the nighttime deposition velocity of SO_2 was found to be slightly larger than that of the daytime value. This anomaly may be due to the higher nighttime relative humidity in their chamber and is explored in more detail in Claiborn et al. (10).

The deposition velocities computed from the present work for red spruce were lower than those calculated for the work by Ennis (Table II); however, the general trend of no significant diurnal difference was also observed in these studies. Ennis et al. (12) performed simultaneous exposures of H_2O_2 , O_3 , and SO_2 , so it may be possible that reactions were occurring between these gases. The effects of interactions between individual pollutants (for example, the aqueous-phase reaction between SO_2 and H_2O_2 leading to acidic solutions) on fluxes to vegetation warrants further investigation since they may have implications for the potential harmful effects on vegetation, and they may also provide another potential sink in inner tissues which are largely comprised of water. Van Hove et al. (31) have observed related phenomena for the adsorption of NH_3 and SO_2 on leaf surfaces and have also speculated about the role of reactions occurring between trace gases on the leaf surface.

Surface Deposition vs Stomatal Deposition. Although the Teflon surfaces of the chamber were assumed to be inert to H_2O_2 , we found that the wall losses of gaseous H_2O_2 were significant. Considering the lack of a statistically significant difference in the measured H_2O_2 uptake during light-on and light-off conditions, we hypothesize that H_2O_2 is not truly inert on the outer, waxy, non-stomatal needle surfaces, but may decompose to some extent there as well. Although neither the rate constant nor the mechanism for the decomposition of gaseous H_2O_2 on the needle cuticular wax is known, we can estimate the effect of the surface reaction on the deposition near the stomatal region. In the following analysis, we assume that H_2O_2 is at least as reactive on the needle surface as it is on the chamber walls, so that the rate constant for the decomposition on needle nonstomatal surfaces is at least as high as that for the wall loss reaction. The amount of gaseous H_2O_2 lost to the cuticular surface is then calculated by treating the losses to the outer needle surfaces and the losses in the stomatal zone as parallel reactions, similar to the procedure for considering the wall losses (24). In this case, the fractional loss to the cuticular surface of the leaf (LL) is calculated from the total leaf area (A_L), the ideal chamber residence time (τ), and the average pseudo-second-order reaction rate constant that is estimated from the wall loss rate constant

$$\text{LL} = \frac{k'_1 A_L \tau}{1 + k'_1 A_L \tau} \quad (5)$$

where k'_1 is the average pseudo-second-order reaction rate constant for the decomposition on cuticular surfaces ($\text{cm}^{-2} \text{min}^{-1}$), assumed to be equal to the average value for the reaction at the chamber walls. Average values for k'_1 were calculated for daytime and nighttime cases. The results of this analysis are presented in Table III. For each experimental run conducted on spruce, the fractional loss to the branches (BL) is decomposed into the fractional loss to the cuticular surface (LL) and a residual that is

Table III. Fractional Losses of Gaseous Hydrogen Peroxide to Needle Nonstomatal and Stomatal Regions for Some Early Experimental Runs on Red Spruce^a

τ (min)	n	av k'_1 ($\text{cm}^{-2} \text{min}^{-1}$)	SL/BL	stomatal flux ($\text{mol cm}^{-2} \text{s}^{-1}$) ($\times 10^{15}$)
Days				
1.0	2	1.394×10^{-5}	0.29 ± 0.02	3.14 ± 1.53
1.3	15	1.394×10^{-5}	0.36 ± 0.33	2.25 ± 2.09
1.6	5	1.394×10^{-5}	0.26 ± 0.26	1.89 ± 1.74
2.1	5	1.394×10^{-5}	0.70 ± 0.21	8.01 ± 3.01
overall, days			0.40 ± 0.26	3.54 ± 2.57
Nights				
1.0	2	4.591×10^{-6}	0.83 ± 0.02	7.65 ± 1.80
1.3	15	4.591×10^{-6}	0.73 ± 0.24	4.98 ± 2.80
1.6	4	4.591×10^{-6}	0.58 ± 0.40	6.21 ± 4.59
2.1	5	4.591×10^{-6}	0.69 ± 0.23	7.92 ± 3.45
overall, nights			0.83 ± 0.06	7.53 ± 3.95

^a τ is the residence time; n is the number of runs; k'_1 is the average pseudo-second-order reaction rate constant for the decomposition on cuticular surfaces, assumed to be equal to average value for the reaction at the chamber walls; SL is the fractional loss to the stomatal region only; BL is the fractional loss to all branch surfaces; and the stomatal flux is the flux of hydrogen peroxide to the stomatal region, only.

assumed to be the fractional loss to the stomatal region. The stomatal loss, SL, is calculated from the total branch loss and the cuticular surface loss

$$SL = \frac{BL - LL}{1 - LL} \quad (6)$$

The stomatal flux, Q_{ST} , (per unit leaf area) is calculated from the fractional loss to the stomatal region (SL)

$$Q_{ST} = \frac{(SL)(F)C_{A_0,exp}}{A_L} \times \text{conversion factors} \quad (7)$$

Since the conifer needle has a porous antechamber located above the stomatal pore, the stomatal flux in this case does not necessarily reflect the mass rate of H_2O_2 that reaches the stomata itself, but represents the mass rate that reaches the antechamber. In Table III, a summary of the calculated stomatal loss for this database is estimated using values for k'_1 that, in turn, are estimated from the average chamber wall losses for daytime and nighttime. Based on this assumption, the flux to the stomatal region varies from 0 to $9.2 \times 10^{-15} \text{ mol cm}^{-2} \text{ s}^{-1}$ (mean $7.53 \pm 3.95 \times 10^{-15} \text{ mol cm}^{-2} \text{ s}^{-1}$) for light-off conditions (24). For light-on runs, the stomatal component of the flux varies from 0 to $12.4 \times 10^{-15} \text{ mol cm}^{-2} \text{ s}^{-1}$ (mean $3.54 \pm 2.57 \times 10^{-15} \text{ mol cm}^{-2} \text{ s}^{-1}$). For comparison, the total flux to the branches as previously calculated is included in this column. As estimated by this method, the stomata contributed on the average $40 \pm 26\%$ to the total flux to the needles for periods when the light was on and $71 \pm 25\%$ when the light was off (Figure 8). Because of the high degree of variability in the wall loss rate constant, this estimate is also highly variable. This calculation suggests that the nighttime stomatal flux of H_2O_2 could actually be higher than that for the daytime, although there is a large degree of uncertainty associated with these estimates.

V. Summary and Conclusions

We have presented the results of a study during which a MFC was utilized to study the flux of H_2O_2 (a very reactive and water-soluble atmospheric trace gas) to

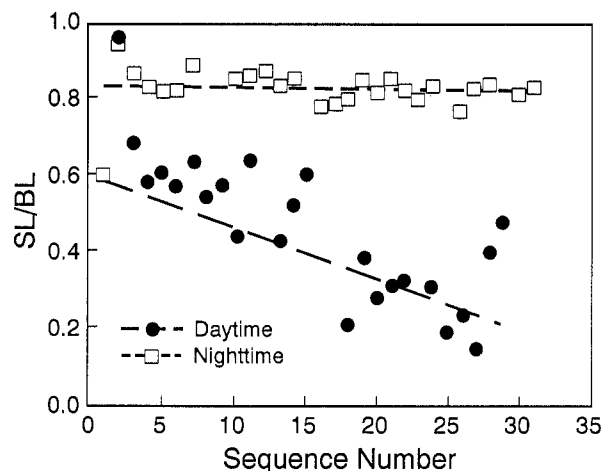


Figure 8. Fraction of the total flux to red spruce needles which is estimated to be to the stomatal region. Ratio of stomatal flux to total leaf flux for each run, in chronological order. Filled circles denote daytime runs (light-on); open squares denote nighttime runs (light-off). Lower limit for non-stomatal flux was estimated using average apparent pseudo-second-order rate constant for decomposition of gaseous hydrogen peroxide on chamber wall surfaces. Upper limit to stomatal flux was estimated by then calculating the residual flux. For light-off conditions, this ratio averaged $83 \pm 6\%$, and for light-on conditions, the ratio averaged $40 \pm 26\%$.

branches of red spruce saplings. Despite the use of inert surfaces in the construction of the chamber, wall losses of gaseous H_2O_2 were significant and highly variable, particularly during the early experiments. It appears that the walls became "conditioned" as the experiment proceeded, and the later wall losses were more consistent. For the later wall losses, the overall apparent reaction rate at the wall did not appear to be first-order with respect to H_2O_2 as originally assumed, but rather varied with the chamber H_2O_2 concentration raised to the -0.56 to -0.57 power. The fractional power may suggest that the reaction mechanism for decomposition proceeds through the formation of an intermediate species (e.g., a radical species such as OH). The actual kinetics of the decomposition of H_2O_2 on wall surfaces should be further investigated in order to improve the accuracy of the flux calculations from uptake experiments such as these.

The difference between the daytime and nighttime deposition velocity for H_2O_2 to red spruce was not found to be statistically significant. The average deposition velocity as measured in these experiments ranged from 0.08 to 0.12 cm s^{-1} for the daytime, and from 0.08 to 0.11 cm s^{-1} for the nighttime experiments. Overall, the average daytime deposition velocity was $0.096 \text{ cm s}^{-1} \pm 40\%$, and the average nighttime deposition velocity was $0.090 \text{ cm s}^{-1} \pm 21\%$.

From these experiments and from the results of preliminary modeling studies presented in the following paper (10) in which these experiments and those of Ennis et al. (12) are interpreted, we conclude that, in these experiments, the losses of H_2O_2 to red spruce had a large contribution due to surface deposition, and that little, if any, gaseous H_2O_2 actually reached the stomata. It is premature to conclude, based on these studies alone, that gas-phase H_2O_2 does not represent a threat to vegetation health. An upper limit to the H_2O_2 flux which is attributed to the entire stomatal region (including the top of the waxy antechamber) was estimated to be $48 \pm 26\%$ of the total flux to needle surfaces during light-on conditions and $73 \pm 24\%$ during light-off conditions. For broadleaf

plants that do not have a sunken stomata like conifers do, it may be likely that H₂O₂ may reach the stomata and even the inner tissues. Further investigation on the uptake of H₂O₂ by species which do not have the stomatal antechamber is warranted to determine if this gas can reach the inner surfaces.

Acknowledgments

This research has been funded in part by the North Carolina State University Air Quality Research Program, USDA-ARS, through which facilities in the NCSU phytotron were made available. We also gratefully acknowledge support made available to C.S.C. in the form of an assistantship from the Department of Chemical Engineering at NCSU. We express sincere appreciation to Dr. Christine Ennis, National Center for Atmospheric Research, for numerous helpful discussions of this experiment; to John Dunning and Bob Philbeck of the USDA for their assistance in the design and construction of the chamber; to Drs. Walter Heck and Richard Reinert of the USDA and Drs. Down and Thomas, NCSU, for lab and greenhouse spaces; to Dr. Hugo Rogers (Auburn University) for the loan of his chamber equipment; and to the U.S. Forest Service Experimental Station in Durham, NH, for providing us the biological materials used in this study. We also thank the anonymous reviewers, whose constructive comments were very helpful.

Notations

A_L	leaf (or needle) surface area, cm ²
BL	fractional loss of pollutant to vegetative surfaces on branches
C_A	pollutant concentration in chamber (measured at outlet), ppb
C_{A_0}	pollutant concentration in feed to chamber (measured at inlet), ppb
CL	fractional loss of pollutant to chamber walls
F	chamber airflow rate, slpm
k_1	pseudo-first-order reaction rate constant for loss to chamber surfaces, min ⁻¹
k_2	pseudo-first-order reaction rate constant for loss to branch surfaces, min ⁻¹
k'_1	pseudo-second-order reaction rate constant for loss to chamber surfaces, cm ⁻² min ⁻¹
k'_2	pseudo-second-order reaction rate constant for loss to branch surfaces, cm ⁻² min ⁻¹
LL	fractional loss of pollutant to cuticular surfaces
Q_A	flux of pollutant (H ₂ O ₂) to branches
Q_{ST}	flux of pollutant (H ₂ O ₂) to stomatal region, only (per cm ² of leaf area)
R	mass-transfer resistance (inverse of deposition velocity), s cm ⁻¹
SL	fractional loss of pollutant to stomatal surfaces (i.e., noncuticular areas)
TL	fractional loss of pollutant to all surfaces (chamber walls plus vegetative surfaces)
V_d	deposition velocity, cm s ⁻¹
τ	residence time, min

Literature Cited

- Siccama, T. G.; Bliss, M.; Vogelmann, H. W. *Bull. Torrey Bot. Club* 1982, 109, 162.
- Johnson, H. T.; Siccama, T. G. *Environ. Sci. Technol.* 1983, 17, 294.
- McLaughlin, S. B. *JAPCA* 1985, 35, 512.
- Bruck, R. I.; Robarge, W. P.; McDaniel, A. *Water, Air, Soil Pollut.* 1989, 48, 161.
- Woodman, J. N.; Cowling, E. B. *Environ. Sci. Technol.* 1987, 21, 120.
- Sakugawa, H.; Kaplan, I. R.; Tsai, W.; Cohen, Y. *Environ. Sci. Technol.* 1990, 24, 1452.
- Claiborn, C. S.; Aneja, V. P. *J. Geophys. Res.* 1991, 96, 18771.
- Lind, J. A.; Kok, G. L. *J. Geophys. Res.* 1986, 91, 7889.
- Chameides, W. L. *J. Geophys. Res.* 1984, 89, 4739.
- Claiborn, C. S.; Carbonell, R. G.; Aneja, V. P. *Environ. Sci. Technol.* 1993, following paper in this issue.
- Masuch, G.; Kettrup, A.; Mallant, R. K. A. M.; Slanina, J. *Int. J. Environ. Anal. Chem.* 1986, 27, 183.
- Ennis, C. A.; Lazrus, A. L.; Zimmerman, P. R.; Monson, R. K. *Tellus* 1990, 42B, 183.
- Hanson, P. J.; McLaughlin, S. B. *J. Environ. Qual.* 1989, 18, 499.
- Enders, G.; Dlugi, R.; Steinbrecher, R.; Clement, B.; Daiber, R.; Eijk, J. V.; Gab, S.; Haziza, M.; Helas, G.; Herrmann, U.; Kessel, M.; Kesselmeier, J.; Kotzias, D.; Kourtidis, K.; Kurth, H.-H.; McMillen, R. T.; Roeder, G.; Schurmann, W.; Teichmann, U.; Torres, L. *Atmos. Environ.* 1992, 26A, 171.
- Rogers, H. H.; Jeffries, H. E.; Stahel, E. P.; Heck, W. W.; Ripperton, L. A.; Witherspoon, A. M. *JAPCA* 1977, 27, 1192.
- Uhl, V. W.; Gray, J. B., Eds. *Mixing: Theory and Practice*; Academic Press: New York, 1966; Vols. I and II.
- Baldocchi, D. B.; Hicks, B. B.; Camara, P. *Atmos. Environ.* 1987, 21, 91.
- Downs, R. J.; Thomas, J. F. *Phytotron Procedural Manual for Controlled Environment Research at the Southeastern Plant Environment Laboratory, North Carolina State University, North Carolina Agricultural Research Service Technical Bulletin 244*, 1983.
- Lazrus, A. L.; Kok, G. L.; Lind, J. A.; Gitlin, S. N.; Heikes, B. G.; Shetter, R. E. *Anal. Chem.* 1986, 58, 594.
- Thompson, F. B.; Leyton, L. *Nature* 1971, 229, 572.
- Drew, A. P.; Running, S. W. *For. Sci.* 1975, 21, 231.
- Koppel, A. T.; Frey, J. M. *Fiziol. Rast.* 1984, 31, 1000.
- Ennis, C. A.; Lazrus, A. L.; Kok, G. L.; Zimmerman, P. R. *Tellus* 1990, 42B, 170.
- Claiborn, C. S. Ph.D. Thesis, North Carolina State University, Raleigh, NC, 1991.
- Bennett, J. H.; Hill, A. C.; Gates, D. M. *JAPCA* 1973, 23, 957.
- Finlayson-Pitts, B. J.; Pitts, J. N., Jr. *Atmospheric Chemistry: Fundamentals and Experimental Techniques*; J. Wiley: New York, 1986.
- Hill, C. G., Jr. *An Introduction to Chemical Engineering Kinetics and Reactor Design*; J. Wiley: New York, 1977.
- Kleinman, L. I. *J. Geophys. Res.* 1986, 91, 10889.
- Trainer, M.; Hsie, E. Y.; McKeen, S. A.; Tallamraju, R.; Parrish, D. D.; Fehsenfeld, F. C.; Liu, S. C. *J. Geophys. Res.* 1987, 92, 11879.
- Rogers, H. H.; Aneja, V. P. *Environ. Exp. Bot.* 1980, 20, 251.
- Van Hove, L. W. A.; Adema, E. H.; Vredenberg, W. J.; Pieters, G. A. *Atmos. Environ.* 1989, 23, 1479.
- Jeffree, C. E.; Johnson, R. P. C.; Jarvis, P. G. *Planta* 1971, 98, 1.
- Taylor, G. E., Jr.; McLaughlin, S. B., Jr.; Shriner, D. S.; Ielvidge, W. J. *Atmos. Environ.* 1983, 17, 789.
- Ennis, C. A. 84th Annual Meeting of the AWMA, Vancouver, June 16-21, 1991, Paper 91-127.3.

Received for review May 25, 1993. Accepted June 23, 1993.*

* Abstract published in *Advance ACS Abstracts*, August 15, 1993.